PERGAMON

Vision Research 42 (2002) 1727–1738

Vision Research

www.elsevier.com/locate/visres

The spatial properties of opponent-motion normalization

Stéphane J.M. Rainville [a,*,1], Nicholas E. Scott-Samuel [b,2], Walter L. Makous [a]

[a] *Center for Visual Science, Meliora 274, University of Rochester, Rochester, NY 14627, USA*
[b] *McGill Vision Research Unit, 687 Pine Ave W., Rm. H4-14, Montréal, Que., Canada H3A 1A1*

Received 8 October 2001; received in revised form 19 April 2002

Abstract

The final stage of the Adelson–Bergen model [J. Opt. Soc. Am. A 2 (1985) 284] computes net motion as the difference between directionally opposite energies E_L and E_R. However, Georgeson and Scott-Samuel [Vis. Res. 39 (1999) 4393] found that human direction discrimination is better described by *motion contrast* (C_m)—a metric where opponent energy ($E_L - E_R$) is divided by flicker energy ($E_L + E_R$). In the present paper, we used a lateral masking paradigm to investigate the spatial properties of flicker energy involved in the normalization of opponent energy. Observers discriminated between left and right motion while viewing a checkerboard in which half of the checks contained a drifting sinusoid and the other half contained flicker (i.e. a counterphasing sinusoid). The relative luminance contrasts of flicker and motion checks determined the checkerboard's overall motion contrast C_m. We obtained selectivity functions for opponent-motion normalization by measuring C_m thresholds whilst varying the orientation, spatial frequency, or size of flicker checks. In all conditions, performance (percent correct) decayed lawfully as we decreased motion contrast, validating the C_m metric for our stimuli. Thresholds decreased with check size and also improved as we increased either the orientation or spatial-frequency difference between motion and flicker checks. Our data are inconsistent with Heeger-type normalization models [Vis. Neurosci. 9 (1992) 181] in which excitatory inputs are normalized by a non-selective pooling of inhibitory inputs, but data are consistent with the implicit assumption in Georgeson and Scott-Samuel's model that flicker normalization is localized in orientation, scale, and space. However, our lateral masking paradigm leaves open the possibility that the spatial properties of flicker normalization would be different if opponent and flicker energies spatially overlapped. Further characterization of motion contrast will require models of the spatial, temporal, and joint space–time properties of mechanisms mediating opponent-motion and flicker normalization.

Keywords: Motion; Flicker; Opponency; Normalization; Contrast; Energy; Direction selectivity; Gain; Center-surround; Lateral masking

1. Introduction

Energy models have had a significant impact on our current understanding of low-level motion perception. Instead of explicitly encoding—or "tracking"—the position of features over time, energy models rely on linear filters sensitive to contours oriented in the space–time domain. Several variants of the energy model, including modified Reichardt detectors (van Santen & Sperling, 1984), have been proposed (Adelson & Bergen, 1985; Burr & Ross, 1986; Watson & Ahumada, 1985) and constitute the basis of other more elaborate models of perceived motion (Qian, Andersen, & Adelson, 1994b; Simoncelli & Heeger, 1998; Wilson, Ferrera, & Yo, 1992).

Fig. 1A sketches the Adelson and Bergen (1985) motion energy model which processes a time-varying luminance input $I(x,t)$ in several stages: (i) input decomposition with pairs of linear spatial and temporal filters in quadrature phase (giving A, A', B, and B'), (ii) linear combination of filter responses into four quadrature components oriented in space–time (giving $A - B'$, $A' + B$, $A + B'$, and $A' - B$), (iii) squaring and summing of quadrature components into directionally opposite energies E_L and E_R, and (iv) subtraction of E_L and E_R at the opponent-motion stage. The various stages of the Adelson–Bergen model are neurally plausible, and most

* Corresponding author. Tel.: +416-736-5659; fax: +416-736-5857.
E-mail address: rainville@hpl.crestech.ca (S.J.M. Rainville).
[1] Present address: Center for Vision Research, York University, 4700 Keele Street, North York, Ont., Canada M3J 1P3.
[2] Present address: Department of Experimental Psychology, University of Bristol, 8 Woodland Road, Bristol BS8 1TN, UK.

0042-6989/02/$ - see front matter
PII: S0042-6989(02)00108-6

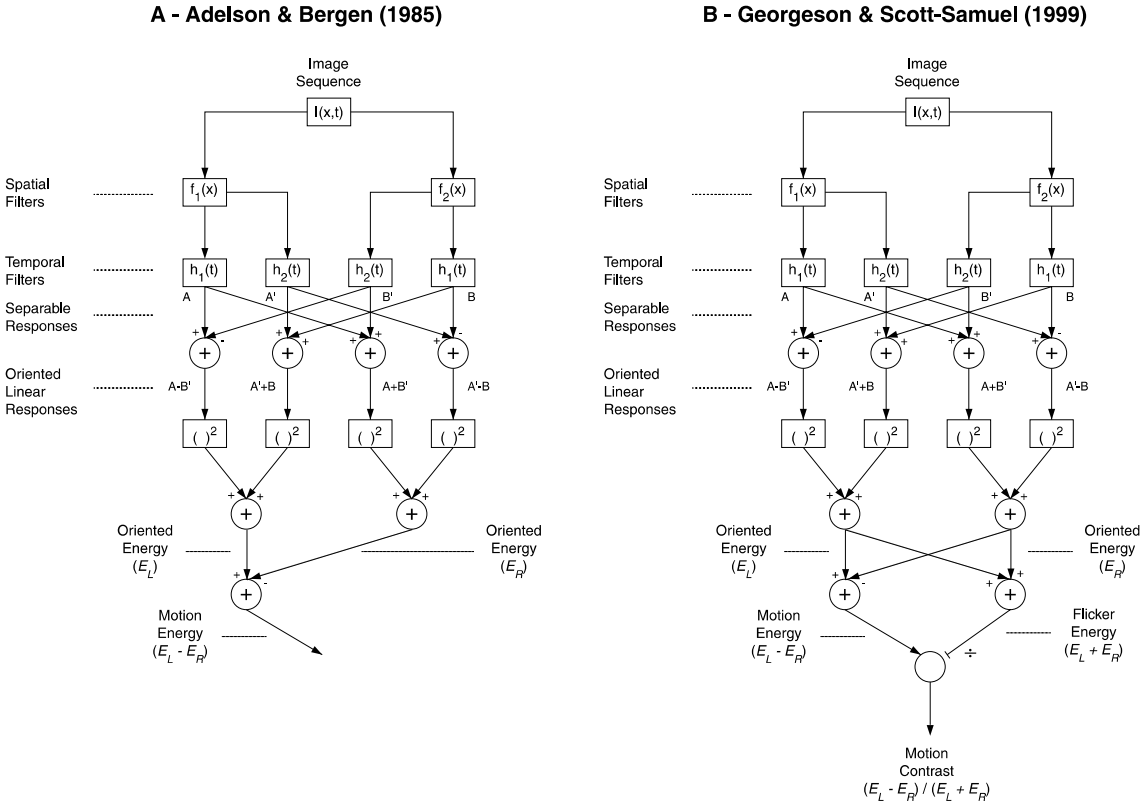

Fig. 1. Motion energy models: A—Schematic illustration of the Adelson and Bergen (1985) motion energy model. The last stage computes motion energy as the difference between directionally opposite energies. B—Schematic illustration of modifications proposed by Georgeson and Scott-Samuel (1999) where motion energy is normalized by flicker energy.

can be mapped to known physiological mechanisms (De Valois, Cottaris, Mahon, Elfar, & Wilson, 2000; Emerson, Bergen, & Adelson, 1992; Heeger, Boynton, Demb, Seidemann, & Newsome, 1999; Hubel & Wiesel, 1968; McLean & Palmer, 1989; McLean, Raab, & Palmer, 1994; Pollen & Ronner, 1981).

Several properties of energy models are consistent with psychophysical data. For instance, the Adelson–Bergen model correctly predicts that a counterphasing grating (i.e. two sinewaves of equal contrasts drifting in opposite directions) elicits a percept of flicker rather than of motion transparency because directionally opposite energies cancel at the opponent stage (Levinson & Sekuler, 1975; Lindsey & Todd, 1998; Mather & Moulden, 1983; Qian, Andersen, & Adelson, 1994a; Stromeyer, Kronauer, Madsen, & Klein, 1984; Zemany, Stromeyer, Chaparro, & Kronauer, 1998), although see Gorea, Conway, and Blake (2001) and Raymond and Braddick (1996). Since the opponent stage computes the difference between directionally opposite energies, the Adelson–Bergen model is insensitive to the absolute amount of spatiotemporal energy in the stimulus.

By analogy with Michelson luminance contrast, Georgeson and Scott-Samuel (1999) have proposed *motion contrast*: a metric denoted by C_{m} that normalizes motion energy $(E_{\mathrm{L}} - E_{\mathrm{R}})$ by flicker energy $(E_{\mathrm{L}} + E_{\mathrm{R}})$. The numerator is identical to the opponent stage of the Adelson–Bergen model, and flicker energy is computed as the sum of directionally opposite energies. One can also think of flicker energy as the total energy let through by the spatiotemporal passband of filters in the Adelson–Bergen model. Implementation of the Georgeson and Scott-Samuel flicker-normalization model is sketched in Fig. 1B.

To validate their motion-contrast metric psychophysically, Georgeson and Scott-Samuel (1999) tested human direction discrimination for a stimulus which can be represented as two superimposed sinewave gratings drifting in opposite directions. Omitting mean luminance for clarity, the authors' time-varying stimuli $I(x,t)$ are described by

$$I(x,t) = c_0 \sin(ux + wt) + c_1 \sin(ux - wt), \qquad (1)$$

where u and w are the spatial and temporal frequencies respectively. Independent control over the contrast of each grating, c_0 and c_1, allows motion contrast to be varied: absolute values of c_0 and c_1 determine overall flicker energy whereas relative values of c_0 and c_1 specify motion energy. Data revealed that direction discrimination increases monotonically with motion contrast but bears no lawful relation to either opponent-motion energy or flicker energy alone.

Inspection of Fig. 1B reveals that the excitatory (i.e. opponent energy) and inhibitory (i.e. flicker energy) components of the Georgeson and Scott-Samuel model have identical spatial properties because both are computed from the same front-end filters, but there is no a priori reason why this must be the case. Motion energy models rely on filters with spatial properties similar to those of early mechanisms of mammalian vision, namely localization in space, orientation, and spatial frequency (DeValois, Albrecht, & Thorell, 1982; DeValois, Yund, & Hepler, 1982; Hubel & Wiesel, 1968). However, as we elaborate further in the Discussion, there is considerable evidence that the response of early visual mechanisms to an optimal test stimulus can be modulated by a masking stimulus whose spatial properties fall outside the classical passband of these mechanisms. Evidence of this non-specific suppression has been incorporated into normalization models where inhibitory pathways are less selective for stimulus properties than excitatory pathways (e.g. Foley, 1994; Heeger, 1992).

1.1. Basic approach

The psychophysical data of Georgeson and Scott-Samuel (1999) cannot be used to distinguish between the spatial properties of the opponent-motion and flicker-normalization stages because motion and flicker energies were spatially superimposed and had the same orientation and spatial frequency. To circumvent this stimulus limitation, we devised a lateral masking paradigm using checkerboard patterns where spatially alternate checks contained either pure flicker or pure motion signals. Holding the spatial properties of motion checks constant, we varied those of flicker checks and measured the extent to which opponent-motion normalization pools across flicker energies of different orientation, scale, or spatial position. Examples of our checkerboard stimuli are shown in Fig. 2 where each check contains a sinewave grating either counterphasing or drifting as a function of time. In these illustrations, counterphasing checks have a high contrast relative to that of motion checks. We manipulated motion contrast, or the ratio of motion energy to flicker energy, by independently controlling the *luminance* contrast of flicker and motion checks. In panel A, motion and flicker checks have the same spatial properties whereas in panels B and C, flicker checks vary in spatial frequency and orientation respectively. Panel D illustrates checks of a different size.

The analytical expression of motion contrast for our stimuli is straightforward. As shown by Eq. (1), the stimuli used by Georgeson and Scott-Samuel can be characterized as two sinewaves of independent contrasts drifting in opposite directions. Use of trigonometric identities reveals that the same stimulus can be recast

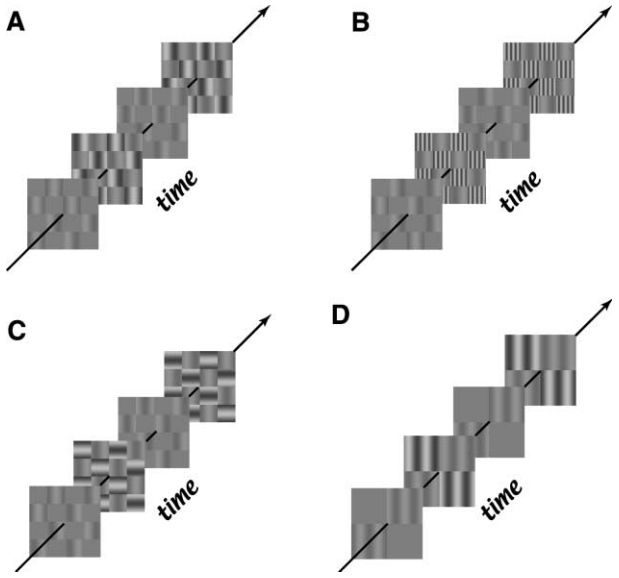

Fig. 2. Checkerboard variant of Georgeson and Scott-Samuel (1999) A—Adjacent checks spatially alternate between flickering and drifting sinewave gratings. Holding the spatial properties of motion checks constant while varying those of flicker checks allowed us to dissociate the spatial properties of opponent-motion and normalization mechanisms. B–D—Flicker checks vary in spatial frequency, orientation, and size respectively.

as the sum of two gratings in spatial and temporal quadrature phase,

$$I(x,t) = m_0 \sin(ux)\cos(wt) + m_1 \cos(ux)\sin(wt), \qquad (2)$$

where $m_0 = (c_0 + c_1)$ and $m_1 = (c_0 - c_1)$. In the case where either m_0 or m_1 is zero, a purely counterphasing grating is obtained whereas setting $m_0 = m_1$ produces a purely drifting grating.

Appendix A in Georgeson and Scott-Samuel (1999) shows that leftward (E_L) and rightward (E_R) energies in the Adelson–Bergen model can be computed easily from Eq. (2): motion energy M is given by

$$M = 4S^2 m_0 m_1, \qquad (3)$$

where S is the gain of the spatiotemporal filters at (u, w), and flicker energy F is obtained by

$$F = 2S^2(m_0^2 + m_1^2). \qquad (4)$$

Recalling that motion contrast, C_m, is defined as M/F, we obtain

$$C_m = \frac{2m_0 m_1}{m_0^2 + m_1^2}. \qquad (5)$$

Opponent energy increases with the product of contrasts m_0 and m_1, and flicker energy increases with the sum of squared contrasts m_0 and m_1. Motion contrast depends only on the luminance contrast ratio m_0/m_1 and is independent of overall contrast energy.

Computing motion contrast for our checkerboard stimuli involves only one additional intermediate step. Since the luminance contrast of motion and flicker

checks can be varied independently, we can reuse Eq. (2) to compute local values of m_0 and m_1 at the individual check level and compute global values of m_0 and m_1 by summing over space. Let us replace m_0 and m_1 by local values d_0 and d_1 for motion checks and by f_0 and f_1 for flicker checks.

According to Eq. (2), pure motion requires that $d_1 = d_0$, and pure flicker requires that either f_0 or f_1 be zero (choosing one or the other to set to zero simply changes the spatiotemporal phase of flicker checks but otherwise does not affect motion contrast). Summing values of m_0 and m_1 over space is simplified given that motion and flicker checks cover equal areas of our stimuli: global values are $m_0 = d_0 + f_0$, and $m_1 = d_1 + f_1$ respectively. Inserting the global values m_0 and m_1 into Eq. (5) returns the motion contrast for our stimuli. Motion contrast is independent of check size, orientation, or scale provided the areas covered by motion and flicker checks are in a one-to-one proportion.

2. Method

2.1. Observers

Two of the authors (SR and NSS), a third informed observer (RH), and two naive observers (LC and AA) participated in the study. All observers had normal or corrected-to-normal vision.

2.2. Hardware and calibration

Experiments were carried out using a Macintosh Powerbook G4/500 (for NSS) and a Macintosh Desktop G4/450 (for all other observers). The two computers hosted standard 8-bit/gun color video cards driving a LaCie Electron 22 Blue monitor (NSS) and a 21″ Apple Studio Display monitor (other observers) respectively. Both displays were set to a spatial resolution of 1152×870 pixels and a refresh rate of 75 Hz. Luminance profiles were measured using a calibrated spot photometer, and grayscale lookup-tables with linear relationships to luminance were derived. After linearization, displays had mean luminances of 33.0 and 29.4 cd/m^2 respectively. Viewing distance was set such that one pixel corresponded to 1′.

2.3. Stimuli

Stimuli consisted of a checkerboard pattern whose checks spatially alternated between drifting and counterphasing sinewave gratings (see Fig. 2). The ''phase'' of the checkerboard was randomized on each trial such that observers could not predict whether a given check would contain motion or flicker. The initial spatial phase of flicker and motion gratings was independently randomized across checks, but initial temporal phase was not, and thus flickering checks reached peak contrast simultaneously. Motion checks invariably consisted of a 1.9 cpd vertical sinusoid (32-pixel period) that drifted either leftwards or rightwards in quadrature steps. Flicker checks were also displayed in quadrature steps and consisted of counterphasing sinusoids of variable spatial frequency and orientation. In all experiments, check size was held fixed at 0.53×0.53 deg (32×32 pixels) with motion checks containing exactly one grating cycle except in Experiment 4 (Fig. 2D) where check size was varied parametrically. Unless otherwise noted, stimuli were composed of 16×16 checks with total dimensions subtending 8.3×8.3 deg (512×512 pixels). Stimuli consisted of five frames presented for a total of 200 ms (or the equivalent of 15 screen refreshes at 75 Hz). Since the first and fifth frames were identical, observers could not infer direction of motion by comparing the initial and final phase of gratings in motion checks. Stimuli were computed in the Matlab 5.2.1 environment and displayed using high-level interfaces from the PsychToolbox (Brainard, 1997) that called lower-level routines from the VideoToolbox (Pelli, 1997).

2.4. Procedure

In all experiments, observers discriminated between left and right motion in a two-alternative forced-choice task and pressed one of two keys to report perceived direction. Levels of motion contrast were presented using the method of constant stimuli and were randomly shuffled across trials. Each run consisted of a variable number of trials depending on the number of conditions to be tested. Although the total number of trials varied across conditions and observers, each data point in Experiment 1 is computed from no less than 50 judgements. Each data point in Experiments 2 through 4 includes no less than 60 judgements.

Stimulus presentations were separated by a variable intertrial interval that depended on the speed at which stimuli were computed and on self-pacing by the observer. A low-contrast fixation dot was shown in the screen's center before every presentation to ensure stimuli were foveated. Observers received auditory feedback on incorrect responses. All thresholds were computed at the 75%-correct level. Error bars (± 1 SD) were computed using a bootstraping technique (Efron & Tibshirani, 1993) that modeled our data as a binary random process. 1000 samples were computed from this process, a $\log x$ cumulative normal was fitted to each sample, and hence a distribution of threshold values was obtained whose standard deviation we took as our confidence interval.

3. Experiment 1: Validating motion contrast for checkerboard stimuli

The purpose of this experiment was to replicate results from Georgeson and Scott-Samuel (1999) with our checkerboard patterns and validate the motion-contrast metric for our stimulus configuration. Observers LC, NSS, RH, and SR participated. Observer performance was measured for all possible combinations of the following luminance contrasts ($d_0 = 2\%$, 4%, 8%, 16%, 32%, and 64%) and motion contrasts ($C_m = 0.062$, 0.125, 0.246, 0.471, 0.8, and 1.0).

Direction discrimination data (proportion correct) are shown in Fig. 3 for all observers as a function of opponent energy (first column), flicker energy (second column), and motion contrast (third column). In line with the findings of Georgeson and Scott-Samuel (1999), performance bears no systematic relationship to either opponent energy ($E_L - E_R$) or flicker energy ($E_L + E_R$) alone but is well described as a monotonic function of motion contrast (C_m). Data in the third column were fitted using a $\log x$ cumulative normal (solid line) and motion-contrast thresholds were estimated at the 75%-correct level. Thresholds were 0.51, 0.42, 0.38, and 0.34 for observers LC, NSS, RH, and SR respectively and are similar to those reported in Georgeson and Scott-Samuel. These results validate the motion-contrast metric for the checkerboard configuration of our stimuli.

4. Experiment 2: Orientation selectivity of opponent-motion normalization

In this experiment, motion-contrast thresholds were measured as a function of the orientation of flicker checks while holding that of motion checks vertical (orientation = 0°). Fig. 2C gives an example of such a stimulus where flicker and motion checks are orthogonal although actual displays contained 16 checks on a side. The luminance contrast of motion checks ($d_0 = d_1$) was fixed at 2%, and motion contrast was varied over the same levels used in Experiment 1. Levels of motion contrast were randomized across trials, and flicker orientation was randomized across runs.

Fig. 4 plots motion-contrast thresholds as a function of flicker orientation for observers AA, LC, NSS, and SR respectively. Solid lines represent the least-squares fit of a three-parameter $\log y$ Gaussian to the data. The fit's peak was constrained to fall on the orientation of motion checks (0°). Selectivity (half bandwidth) was defined as the orientation where thresholds dropped by a factor of two from the highest point on the fitted curve. We chose this criterion to better compare these results with those of experiments in which we fitted data with functions other than Gaussians.

Results show that motion-contrast thresholds drop significantly as the orientation difference between motion and flicker checks increases, but the shape of the data varies across observers. Orientation selectivity for observers AA, LC, NSS, and SR, were 42.0°, 42.0°, 22.5°, and 19.2° respectively. The orientation selectivity of the two informed observers (NSS and SR) is narrower than that of the two naïve observers. Thresholds could not be measured beyond 45° for NSS and SR because performance remained above 75% correct for the range of motion contrasts that were available with our display. Although the orientation selectivity computed for observers AA and LC is identical, most of the threshold reduction occurs between ±45° for AA whereas LC's performance improves more gradually with orientation. It is plausible that naïve observers suffer from greater internal noise than practiced subjects. Since larger internal noise raises threshold, the range of motion contrasts used here may have been sufficient to measure the selectivity of naïve observers over the entire orientation spectrum. Nonetheless, the essential finding is that for each observer, motion-contrast thresholds decay lawfully as a function of the orientation difference between motion and flicker checks.

5. Experiment 3: Spatial-frequency selectivity of opponent-motion normalization

In this experiment, motion-contrast thresholds were measured as a function of the spatial frequency of flicker checks while holding that of motion checks constant at 1.9 cpd. Fig. 2B gives an example of such a stimulus where flicker checks have four times the spatial frequency of motion checks. Actual displays contained 16 checks on a side. The luminance contrast of motion checks ($d_0 = d_1$) was fixed at 2%, and motion contrast was varied over the same levels used in Experiment 1. Levels of motion contrast were randomized across trials, and flicker spatial frequency was randomized across runs.

Fig. 5 plots motion-contrast thresholds as a function of flicker spatial frequency for observers LC, NSS, and SR respectively. Solid lines represent the best (least-squares) fit of a three-parameter log–log Gaussian to the data. We defined selectivity (half bandwidth) as the spatial frequency where thresholds dropped by a factor of two from the highest point on the fitted curve. For all observers, results show that motion-contrast thresholds decay lawfully as the spatial-frequency difference between motion and flicker checks increases. LC, NSS, and SR, have spatial-frequency selectivities of 0.41, 0.45, and 0.66 octaves respectively.

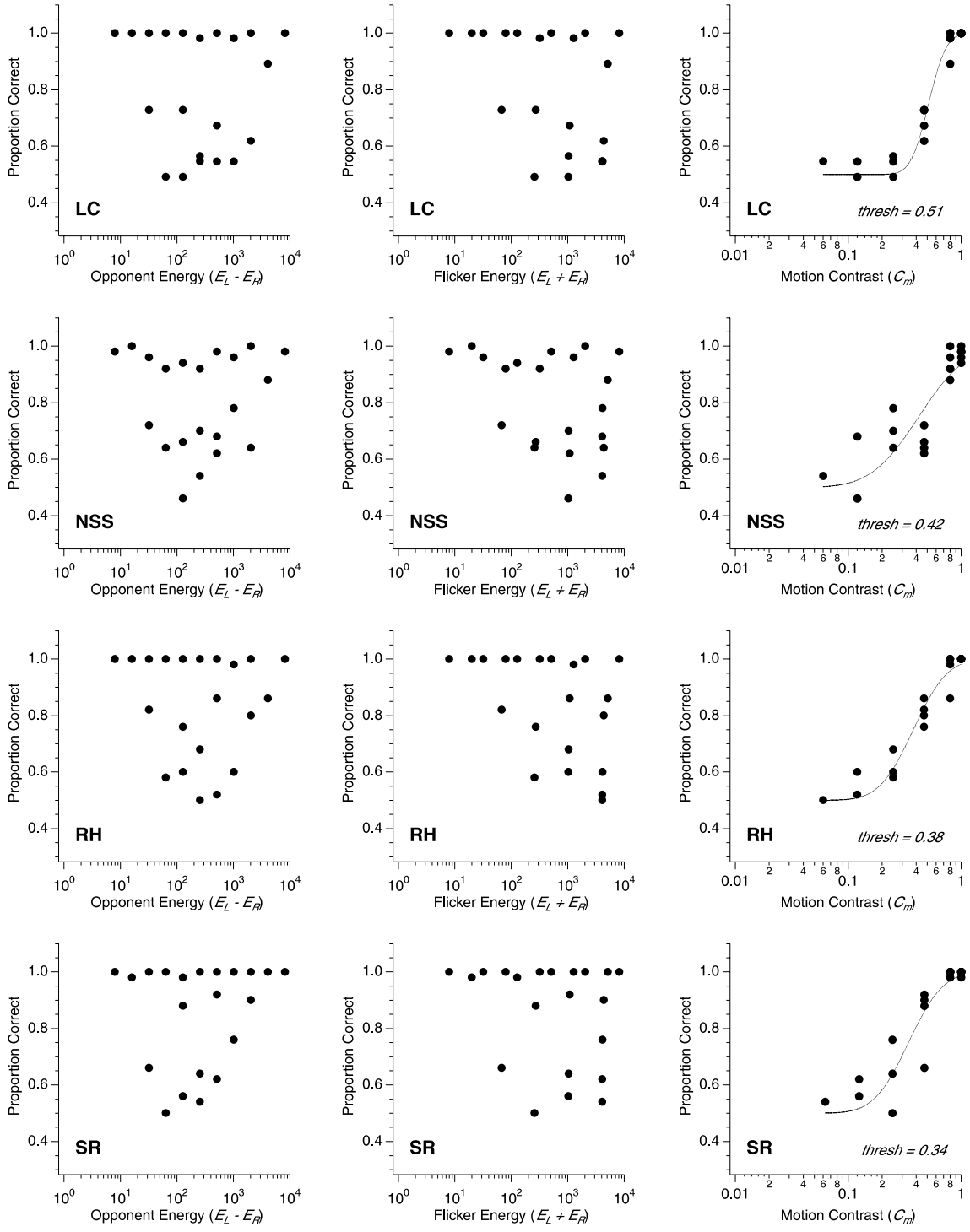

Fig. 3. Three metrics compared: Direction discrimination (proportion correct) vs. opponent energy (first column), flicker energy (second column), and motion contrast (third column) for observers LC, NSS, RH, and SR (rows). Performance vs. motion contrast is fitted with a $\log x$ cumulative normal. Estimates of motion-contrast thresholds are reported at the 75%-correct level.

6. Experiment 4: Spatial selectivity of opponent-motion normalization

In this experiment, motion-contrast thresholds were measured as a function of check size. Motion and flicker checks invariably contained a vertical 1.9 cpd sinewave grating. Panel D of Fig. 2 shows an example of such a stimulus where check dimensions have been doubled from previous figures. Seven different check sizes were used (0.27, 0.53, 0.60, 0.67, 0.80, 1.07, and 1.33 deg on a

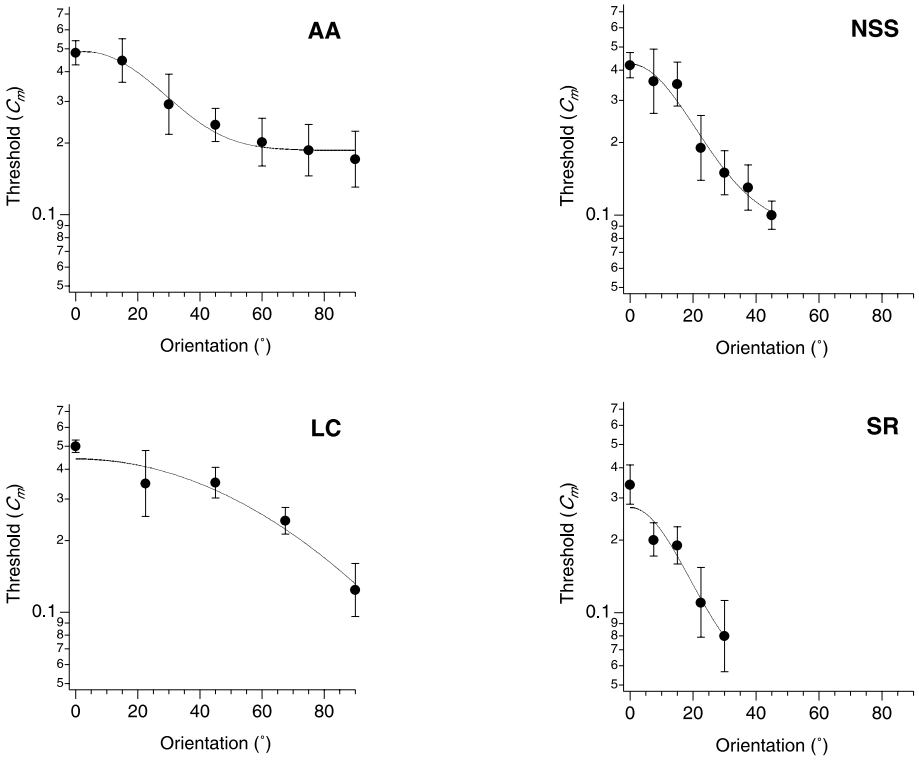

Fig. 4. Orientation selectivity of opponent-motion normalization: Motion-contrast thresholds are plotted as a function of flicker orientation for observers AA, LC, NSS, and SR. Solid lines show the best log y Gaussian fit to the data. Error bars show ±1 SD.

side) although only a subset of the conditions were shown to each observer as dictated by pilot data. To avoid partial checks, stimulus dimensions were adjusted between 8.0 and 8.5 deg such that only complete checks were included; stimulus dimensions corresponding to the 7 check sizes listed above were 8.5, 8.5, 8.4, 8.0, 8.0, 8.5, and 8.0 deg respectively. Although the total number of checks varied across conditions, every stimulus was evenly divided between motion and flicker checks.

The luminance contrast of motion checks $(d_0 = d_1)$ was fixed at 2%, and motion contrast was varied over the same levels used in Experiment 1. Levels of motion contrast were randomized across trials, and check size was randomized across runs.

Fig. 6 plots motion-contrast thresholds as a function of check size for observers LC, NSS, and SR respectively. Solid lines represent the least-squares fit of a four-parameter cumulative normal (with negative slope) to the data. The size of the normalization's pooling area was defined as the check size where thresholds dropped by a factor of two from the highest point on the fitted curve.

For all observers, results show that motion-contrast thresholds decrease rapidly as the size of motion and flicker checks increases. The size of the opponent-motion normalization's pooling area for LC, NSS, and SR is 0.63, 0.30, and 0.30 deg respectively.

7. Summary of results

The present study has produced the following findings:

- Motion contrast is a valid descriptor of human direction discrimination in checkerboard stimuli whose checks spatially alternate between drifting and counterphasing gratings (Experiment 1).
- The normalization of opponent-motion energy is selective for the spatial orientation of flicker energy (Experiment 2).
- The normalization of opponent-motion energy is selective for the spatial frequency of flicker energy (Experiment 3).
- The normalization of opponent-motion energy is selective for the spatial location of flicker energy (Experiment 4).

Table 1 summarizes the selectivity of opponent-motion normalization for orientation, scale, and space as measured empirically for individual observers.

8. Discussion

The main thrust of the present paper lies in the empirical demonstration that opponent-motion normalization,

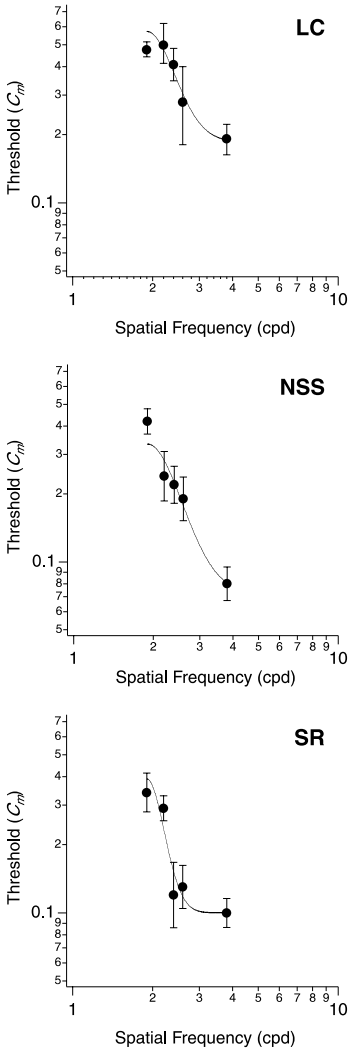

Fig. 5. Spatial-frequency selectivity of opponent-motion normalization: Motion-contrast thresholds are plotted as a function of flicker spatial frequency for observers LC, NSS, and SR. Solid lines show the best log–log Gaussian fit to the data. Error bars show ±1 SD.

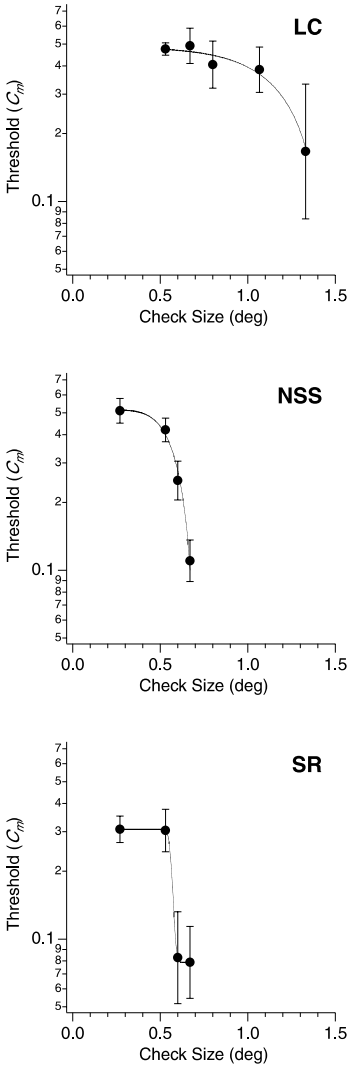

Fig. 6. Spatial selectivity of opponent-motion normalization: Motion-contrast thresholds are plotted as a function of check size for observers LC, NSS, and SR. Solid lines show the best cumulative-normal fit to the data. Error bars show ±1 SD.

as revealed by lateral masking, is selective for the orientation, scale, and location of flicker energy. In the following sections, we discuss the implications of our results and propose directions for future work.

8.1. The spatial properties of opponent-motion normalization

We tested whether or not opponent-motion normalization is selective for the spatial properties of flicker energy. Results summarized in Table 1 show that, despite some quantitative disagreement between naïve observer LC and informed observers NSS and SR, performance is clearly selective for the relative orientation, scale, and location of motion and flicker energies. The orientation and spatial-frequency selectivity of opponent-motion normalization reported in Table 1 are similar to those of direction-selective mechanisms measured in other psychophysical studies on motion perception. Orientation selectivity falls within the range measured by Anderson and Burr (1991), Anderson, Burr, and Morrone (1991) and Georgeson and Scott-Samuel (2000), and selectivity for spatial frequency is

Table 1
The spatial properties of opponent-motion normalization

	Orientation (°)	SF (octaves)	Space (deg)
LC	42.0	0.41	0.63
NSS	22.5	0.45	0.30
SR	22.5	0.66	0.30

Orientation, spatial frequency, and spatial selectivity is shown for individual observers (LC, NSS, and SR). Selectivity for orientation, spatial frequency, and space represent half bandwidths corresponding to a halving of threshold.

consistent with estimates of Anderson and Burr (1989). However, the size of opponent-motion normalization measured in our study is larger than the size of motion mechanisms reported in other studies (Anderson & Burr, 1987; Anderson & Burr, 1991; Anderson et al., 1991; Georgeson & Scott-Samuel, 2000). This larger spatial extent is compatible with the notion that motion opponency arises primarily at the level of MT (Heeger et al., 1999; Qian & Andersen, 1994; van Wezel, Lankheet, Verstraten, Maree, & van de Grind, 1996) where receptive fields are larger than those in direction-selective V1 cells, but we cannot exclude that estimates of size vary across studies due to pitfalls specific to different techniques used (Fredericksen, Verstraten, & van de Grind, 1997). Two obvious sources of such cross-study variability in psychophysical estimates include the arbitrary criterion chosen to define threshold (e.g. 75% correct) and the criterion chosen to define selectivity along a given dimension such as orientation (e.g. a factor-of-two drop from peak threshold).

8.2. Lateral vs. superposition masking

There is considerable evidence that mechanisms responding to a mask falling outside their excitatory passband have different spatial properties depending on whether the mask is superimposed on the test or presented laterally. In physiological studies, when test and mask are spatially superimposed, response inhibition is largely non-selective for mask orientation (Bonds, 1989; Carandini, Barlow, O'Keefe, Poirson, & Movshon, 1997; Carandini, Heeger, & Movshon, 1997; DeAngelis, Robson, Ohzawa, & Freeman, 1992; Morrone, Burr, & Maffei, 1982; Sengpiel & Blakemore, 1994)—although recent evidence suggests cross-orientation inhibition is not intracortical (Anderson, Carandini, & Ferster, 2000; Carandini, Heeger, & Seen, 2001)—and only broadly tuned for mask spatial frequency (Albrecht & Hamilton, 1982; Bonds, 1989; De Valois & Tootell, 1983; DeAngelis et al., 1992; Morrone et al., 1982). If test and mask are presented laterally, response inhibition becomes more selective for mask orientation (DeAngelis, Freeman, & Ohzawa, 1994; Levitt & Lund, 1997; Li, Thier, & Wehrhahn, 2000; Nelson & Frost, 1978; Nothdurft, Gallant, & van Essen, 1999; Polat, Mizobe, Pettet, Kasamatsu, & Norcia, 1998; Sengpiel, Sen, & Blakemore, 1997; Toth, Rao, Kim, Somers, & Sur, 1996) and spatial frequency (DeAngelis et al., 1994; Li & Li, 1994).

Similar results are found in the psychophysical literature, although selectivity is generally narrower than measured physiologically. If test and mask are spatially superimposed, masking is selective for orientation and spatial frequency (e.g. Phillips & Wilson, 1984; Wilson, McFarlane, & Phillips, 1983), but there is some evidence that superimposed masks that differ significantly from the test can also have inhibitory effects (Foley, 1994; Itti, Koch, & Braun, 2000; Olzak & Thomas, 1992; Snowden & Hammett, 1992). If test and mask are presented laterally, inhibition is generally tuned for orientation and spatial frequency (Cannon & Fullenkamp, 1991; Chubb, Sperling, & Solomon, 1989; Olzak & Laurinen, 1999; Xing & Heeger, 2000). At both the physiological and psychophysical levels, however, the effects of masking are complex (even facilitatory) and depend on the relative spatial properties and contrast levels of masks and tests (Gilbert, Das, Ito, Kapadia, & Westheimer, 1996; Kapadia, Ito, Gilbert, & Westheimer, 1995; Levitt & Lund, 1997; Nelson & Frost, 1985; Polat & Sagi, 1993; Polat & Sagi, 1994), on whether masks and tests are viewed dichoptically (e.g. DeAngelis et al., 1992), and on modulation from attentional processes (Freeman, Sagi, & Driver, 2001; Ishai & Sagi, 1995).

The distinction between mechanisms mediating lateral and superposition masking is important given that in our study, counterphasing gratings were spatially adjacent to—rather than superimposed on—the drifting gratings. Our results are in line with those of previous psychophysical findings on lateral masking, although it remains to be shown whether the mechanisms mediating opponent-motion normalization are the same as those isolated in the spatial vision literature. The key implication of distinguishing between lateral and superposition masking, however, is that it limits the scope of the conclusions we can draw from the present study. Our results are consistent with the Georgeson and Scott-Samuel model in its current form where flicker energy, like motion energy, is derived from the same front-end filters localized in orientation, scale, and space. However, we must leave open the possibility that selectivity for orientation and spatial frequency could be different if flickering masks were superimposed on drifting tests.

8.3. Modeling opponent-motion normalization

Our understanding of mammalian vision has been influenced by models where stimuli are decomposed by a bank of linear filters whose output pass through nonlinear transduction and internal noise before reaching a decision stage (e.g. Legge & Foley, 1980). However, such models are excitatory in nature and cannot explain data where the response of a visual mechanism is affected by masks falling outside its passband. To account for such findings, several authors have proposed divisive gain control schemes in which the response of each mechanism is normalized by the pooled response of mechanisms tuned to other stimulus properties (e.g. Albrecht & Geisler, 1991; Carandini et al., 1997; Foley, 1994; Heeger, 1992; Ross & Speed, 1991; Snowden & Hammett, 1992; Thomas & Olzak, 1997; Watson & Solomon, 1997; Wilson & Humanski, 1993). Heeger's normalization model where inhibitory signals are pooled non-selectively across orientations, scales and positions

has been particularly influential because of its ability to account for a large body of physiological data.

While the localization of flicker normalization in orientation, scale, and space is consistent with the model proposed by Georgeson and Scott-Samuel (1999), our findings cannot be explained by models such as Heeger's in which normalization is strictly non-selective for the spatial properties of the stimulus. In several of the models cited above, however, the pooling of normalization signals is preceded by a broadly tuned function that gives greater inhibitory weight to mechanisms selective for properties similar to the test stimulus. A more quantitative comparison between the spatial properties of mechanisms mediating opponent-motion and flicker normalization would require studying both mechanisms within the same paradigm and inferring their underlying spatial tuning and transducer functions with the help of a psychophysical model that explicitly takes into account the relative spatial tuning of excitatory and inhibitory pathways (e.g. Foley, 1994; Foley & Chen, 1997).

8.4. The joint space–time properties of opponent-motion normalization

As it currently stands, the opponent-motion normalization stage proposed by Georgeson and Scott-Samuel (1999) has no dynamics other than those imposed by the front-end temporal filters of the Adelson–Bergen model. It remains to be determined empirically whether normalization mirrors the temporal properties of these front-end filters or whether it has dynamics of its own. A full characterization of opponent-motion normalization, however, requires not only a better description of its dynamics but also a description of its *joint* spatial and temporal properties. For example, pooling across orientation, scale and space presumably requires integration across (and feedback from) remote cortical loci, and therefore investigating either spatial or temporal properties alone cannot reveal whether normalization becomes spatially more or less selective at time scales other than those used in the present study.

Another incentive for investigating the joint spatiotemporal properties of opponent-motion normalization comes from the properties of receptive fields of cells found in area MT/V5. Current evidence points to MT/V5 as the principal cortical area involved in motion opponency (Heeger et al., 1999; Qian & Andersen, 1994; van Wezel et al., 1996), and cells in MT/V5 have a richer spatiotemporal selectivity than that found in their direction-selective V1 afferents. Several authors have suggested that the space–time inseparable properties of MT/V5 cells effectively solve the aperture problem of direction-selective units—the "oriented energy" stage in the Adelson and Bergen (1985) model—by implementing an approximation to the intersection-of-constraints (Adelson & Movshon, 1982; Albright, 1984; Movshon & Newsome, 1996; Perrone & Thiele, 2001; Simoncelli & Heeger, 1998; Wilson et al., 1992). Recent psychophysical evidence has revealed better summation of spatiotemporal energy when it is distributed on an intersection-of-constraints plane in the Fourier domain (Schrater, Knill, & Simoncelli, 2000). Whether opponent motion is normalized by flicker energy lying on the same plane remains an open issue.

9. Conclusions

The present study has revisited Georgeson and Scott-Samuel's (1999) notion of motion contrast—a metric of human direction discrimination that normalizes opponent-motion energy by flicker energy. We tested two competing hypotheses, namely whether or not the mechanisms involved in flicker normalization are selective for orientation, scale, and position. Our data disagree with non-selective normalization models in which response is divided by the pooled activity of visual mechanisms irrespective of their spatial properties (Carandini et al., 1997; Heeger, 1992) but are consistent with the implicit assumption in Georgeson and Scott-Samuel's model that the normalization stage shares the opponent-motion stage's selectivity for orientation, spatial frequency, and space. However, our data are derived from a lateral masking paradigm and it is currently unknown whether the selectivity of normalization carries over to conditions where flicker and motion spatially overlap. Future studies will need to model the spatial properties of mechanisms underlying the selectivity of opponent-motion and flicker-normalization stages and determine the extent to which they are similar. Additional characterization of opponent-motion normalization will require data and modeling on its dynamics as well as on its joint spatiotemporal properties.

Acknowledgements

This research was supported by grants EY-4885 and EY-1319, and by Medical Research Council of Canada grant MT10818 awarded to Robert Hess. SR is also supported by a post-doctoral fellowship from the Natural Science and Engineering Council of Canada. Part of this research has been published as a conference abstract (Rainville, Scott-Samuel, Makous, & Hess, 2001).

References

Adelson, E. H., & Bergen, J. (1985). Spatio-temporal energy models for the perception of motion. *Journal of the Optical Society of America, 2*, 284–299.

Adelson, E. H., & Movshon, J. A. (1982). Phenomenal coherence of moving visual patterns. *Nature, 300*(5892), 523–525.

Albrecht, D. G., & Geisler, W. S. (1991). Motion selectivity and the contrast-response function of simple cells in the visual cortex. *Visual Neuroscience, 7*(6), 531–546.

Albrecht, D. G., & Hamilton, D. B. (1982). Striate cortex of monkey and cat: Contrast response function. *Journal of Neurophysiology, 48*(1), 217–237.

Albright, T. D. (1984). Direction and orientation selectivity of neurons in visual area MT of the macaque. *Journal of Neurophysiology, 52*(6), 1106–1130.

Anderson, J. S., Carandini, M., & Ferster, D. (2000). Orientation tuning of input conductance, excitation, and inhibition in cat primary visual cortex. *Journal of Neurophysiology, 84*(2), 909–926.

Anderson, S. J., & Burr, D. C. (1987). Receptive field size of human motion detection units. *Vision Research, 27*(4), 621–635.

Anderson, S. J., & Burr, D. C. (1989). Receptive field properties of human motion detector units inferred from spatial frequency masking. *Vision Research, 29*(10), 1343–1358.

Anderson, S. J., & Burr, D. C. (1991). Spatial summation properties of directionally selective mechanisms in human vision. *Journal of the Optical Society of America A Optics & Image Science, 8*(8), 1330–1339.

Anderson, S. J., Burr, D. C., & Morrone, M. C. (1991). Two-dimensional spatial and spatial-frequency selectivity of motion-sensitive mechanisms in human vision. *Journal of the Optical Society of America A Optics & Image Science, 8*(8), 1340–1351.

Bonds, A. B. (1989). Role of inhibition in the specification of orientation selectivity of cells in the cat striate cortex. *Visual Neuroscience, 2*(1), 41–55.

Brainard, D. H. (1997). The Psychophysics Toolbox. *Spatial Vision, 10*, 443–446.

Burr, D. C., & Ross, J. (1986). Visual processing of motion. *Trends in Neuroscience, 9*, 304–306.

Cannon, M. W., & Fullenkamp, S. C. (1991). Spatial interactions in apparent contrast: inhibitory effects among grating patterns of different spatial frequencies, spatial positions and orientations. *Vision Research, 31*(11), 1985–1998.

Carandini, M., Barlow, H. B., O'Keefe, L. P., Poirson, A. B., & Movshon, J. A. (1997). Adaptation to contingencies in macaque primary visual cortex. *Philosophical Transactions of the Royal Society of London Series B: Biological Sciences, 352*(1358), 1149–1154.

Carandini, M., Heeger, D. J., & Movshon, J. A. (1997). Linearity and normalization in simple cells of the macaque primary visual cortex. *Journal of Neuroscience, 17*(21), 8621–8644.

Carandini, M., Heeger, D. J., & Seen, W. (2001). Cross-orientation suppression in V2 explained by synaptic depression. *Soc. Neurosci. Abstr, 27*(572.14).

Chubb, C., Sperling, G., & Solomon, J. A. (1989). Texture interactions determine perceived contrast. *Proceedings of the National Academy of Sciences of the United States of America, 86*(23), 9631–9635.

DeAngelis, G. C., Robson, J. G., Ohzawa, I., & Freeman, R. D. (1992). Organization of suppression in receptive fields of neurons in cat visual cortex. *Journal of Neurophysiology, 68*(1), 144–163.

DeAngelis, G. C., Freeman, R. D., & Ohzawa, I. (1994). Length and width tuning of neurons in the cat's primary visual cortex. *Journal of Neurophysiology, 71*(1), 347–374.

DeValois, R. L., Albrecht, D. G., & Thorell, L. G. (1982a). Spatial frequency selectivity of cells in macaque visual cortex. *Vision Research, 22*, 545–559.

DeValois, R. L., Yund, E. W., & Hepler, N. (1982b). The orientation and direction selectivity of cells in macaque visual cortex. *Vision Research, 22*, 531–544.

De Valois, K. K., & Tootell, R. B. (1983). Spatial-frequency-specific inhibition in cat striate cortex cells. *Journal of Physiology, 336*, 359–376.

De Valois, R. L., Cottaris, N. P., Mahon, L. E., Elfar, S. D., & Wilson, J. A. (2000). Spatial and temporal receptive fields of geniculate and cortical cells and directional selectivity. *Vision Research, 40*(27), 3685–3702.

Efron, B., & Tibshirani, R. J. (1993). *An introduction to the bootstrap*. New York: Chapman & Hall.

Emerson, R. C., Bergen, J. R., & Adelson, E. H. (1992). Directionally selective complex cells and the computation of motion energy in cat visual cortex. *Vision Research, 32*(2), 203–218.

Foley, J. M. (1994). Human luminance pattern-vision mechanisms: masking experiments require a new model. *Journal of the Optical Society of America A Optics & Image Science, 11*(6), 1710–1719.

Foley, J. M., & Chen, C. C. (1997). Analysis of the effect of pattern adaptation on pattern pedestal effects: a two-process model. *Vision Research, 37*(19), 2779–2788.

Fredericksen, R. E., Verstraten, F. A., & van de Grind, W. A. (1997). Pitfalls in estimating motion detector receptive field geometry. *Vision Research, 37*(1), 99–119.

Freeman, E., Sagi, D., & Driver, J. (2001). Lateral interactions between targets and flankers in low-level vision depend on attention to the flankers. *Nature Neuroscience, 4*(10), 1032–1036.

Georgeson, M. A., & Scott-Samuel, N. E. (1999). Motion contrast: a new metric for direction discrimination. *Vision Research, 39*, 4393–4402.

Georgeson, M. A., & Scott-Samuel, N. E. (2000). Spatial resolution and receptive field height of motion sensors in human vision. *Vision Research, 40*(7), 745–758.

Gilbert, C. D., Das, A., Ito, M., Kapadia, M., & Westheimer, G. (1996). Spatial integration and cortical dynamics. *Proceedings of the National Academy of Sciences of the United States of America, 93*(2), 615–622.

Gorea, A., Conway, T. E., & Blake, R. (2001). Interocular interactions reveal the opponent structure of motion mechanisms. *Vision Research, 41*(4), 441–448.

Heeger, D. J. (1992). Normalization of cell responses in cat striate cortex. *Visual Neuroscience, 9*, 181–197.

Heeger, D. J., Boynton, G. M., Demb, J. B., Seidemann, E., & Newsome, W. T. (1999). Motion opponency in visual cortex. *Journal of Neuroscience, 19*(16), 7162–7174.

Hubel, D. H., & Wiesel, T. N. (1968). Receptive fields and functional architecture of monkey striate cortex. *Journal of Physiology, 195*, 215–243.

Ishai, A., & Sagi, D. (1995). Common mechanisms of visual imagery and perception. *Science, 268*(5218), 1772–1774.

Itti, L., Koch, C., & Braun, J. (2000). Revisiting spatial vision: toward a unifying model. *Journal of the Optical Society of America, A, Optics, Image Science, & Vision, 17*(11), 1899–1917.

Kapadia, M. K., Ito, M., Gilbert, C. D., & Westheimer, G. (1995). Improvement in visual sensitivity by changes in local context: parallel studies in human observers and in V1 of alert monkeys. *Neuron, 15*(4), 843–856.

Legge, G. E., & Foley, J. M. (1980). Contrast masking in human vision. *Journal of the Optical Society of America, 70*(12), 1458–1471.

Levinson, E., & Sekuler, R. (1975). Inhibition and disinhibition of direction-specific mechanisms in human vision. *Nature, 254*(5502), 692–694.

Levitt, J. B., & Lund, J. S. (1997). Contrast dependence of contextual effects in primate visual cortex. *Nature, 387*(6628), 73–76.

Li, C. Y., & Li, W. (1994). Extensive integration field beyond the classical receptive field of cat's striate cortical neurons–classification and tuning properties. *Vision Research, 34*(18), 2337–2355.

Li, W., Thier, P., & Wehrhahn, C. (2000). Contextual influence on orientation discrimination of humans and responses of neurons in V1 of alert monkeys. *Journal of Neurophysiology, 83*(2), 941–954.

Lindsey, D. T., & Todd, J. T. (1998). Opponent motion interactions in the perception of transparent motion. *Perception & Psychophysics, 60*(4), 558–574.

Mather, G., & Moulden, B. (1983). Thresholds for movement direction: two directions are less detectable than one. *Quarterly Journal of Experimental Psychology. A, Human Experimental Psychology, 3*, 513–518.

McLean, J., & Palmer, L. A. (1989). Contribution of linear spatio-temporal receptive field structure to velocity selectivity of simple cells in area 17 of cat. *Vision Research, 29*(6), 675–679.

McLean, J., Raab, S., & Palmer, L. A. (1994). Contribution of linear mechanisms to the specification of local motion by simple cells in areas 17 and 18 of the cat. *Visual Neuroscience, 11*(2), 271–294.

Morrone, M. C., Burr, D. C., & Maffei, L. (1982). Functional implications of cross-orientation inhibition of cortical visual cells. I. Neurophysiological evidence. *Proceedings of the Royal Society of London Series B: Biological Sciences, 216*(1204), 335–354.

Movshon, J. A., & Newsome, W. T. (1996). Visual response properties of striate cortical neurons projecting to area MT in macaque monkeys. *Journal of Neuroscience, 16*(23), 7733–7741.

Nelson, J. I., & Frost, B. J. (1978). Orientation-selective inhibition from beyond the classic visual receptive field. *Brain Research, 139*(2), 359–365.

Nelson, J. I., & Frost, B. J. (1985). Intracortical facilitation among co-oriented, co-axially aligned simple cells in cat striate cortex. *Experimental Brain Research, 61*(1), 54–61.

Nothdurft, H.-C., Gallant, J. L., & van Essen, D. C. (1999). Response modulation by texture surround in primate area V1: Correlates of ''popout'' under anesthesia. *Visual Neuroscience, 16*(1), 15–34.

Olzak, L. A., & Laurinen, P. I. (1999). Multiple gain control processes in contrast–contrast phenomena. *Vision Research, 39*(24), 3983–3987.

Olzak, L. A., & Thomas, J. P. (1992). When orthogonal orientations are not processed independently. *Vision Research, 32*, 1885–1898.

Pelli, D. G. (1997). The VideoToolbox software for visual psychophysics: Transforming numbers into movies. *Spatial Vision, 10*, 437–442.

Perrone, J. A., & Thiele, A. (2001). Speed skills: measuring the visual speed analyzing properties of primate MT neurons. *Nature Neuroscience, 4*(5), 526–532.

Phillips, G. C., & Wilson, H. R. (1984). Orientation bandwidths of spatial mechanisms measured by masking. *Journal of the Optical Society of America A Optics & Image Science, 1*(2), 226–232.

Polat, U., Mizobe, K., Pettet, M. W., Kasamatsu, T., & Norcia, A. M. (1998). Collinear stimuli regulate visual responses depending on cell's contrast threshold. *Nature, 391*(6667), 580–584.

Polat, U., & Sagi, D. (1993). Lateral interactions between spatial channels: Suppression and facilitation revealed by lateral masking experiments. *Vision Research, 33*(7), 993–999.

Polat, U., & Sagi, D. (1994). The architecture of perceptual spatial interactions. *Vision Research, 34*(1), 73–78.

Pollen, D. A., & Ronner, S. F. (1981). Phase relationships between adjacent simple cells in the visual cortex. *Science, 212*, 1409–1411.

Qian, N., & Andersen, R. A. (1994). Transparent motion perception as detection of unbalanced motion signals. II. Physiology. *Journal of Neuroscience, 14*(12), 7367–7380.

Qian, N., Andersen, R. A., & Adelson, E. H. (1994a). Transparent motion perception as detection of unbalanced motion signals. I. Psychophysics. *Journal of Neuroscience, 14*(12), 7357–7366.

Qian, N., Andersen, R. A., & Adelson, E. H. (1994b). Transparent motion perception as detection of unbalanced motion signals: III. Modeling. *Journal of Neuroscience, 14*(12), 7381–7392.

Rainville, S. J. M., Scott-Samuel, N. E., Makous, W. L., & Hess, R. F. (2001). The spatial properties of opponent-motion energy normalization. *Investigative Ophthalmology & Visual Science, 42*(4), S870.

Raymond, J., & Braddick, O. (1996). Responses to opposed directions of motion: continuum or independent mechanisms? *Vision Research, 36*(13), 1931–1937.

Ross, J., & Speed, H. D. (1991). Contrast adaptation and contrast masking in human vision. *Proceedings of the Royal Society of London - Series B: Biological Sciences, 246*(1315), 61–69.

Schrater, P. R., Knill, D. C., & Simoncelli, E. P. (2000). Mechanisms of visual motion detection. *Nature Neuroscience, 3*(1), 64–68.

Sengpiel, F., & Blakemore, C. (1994). Interocular control of neuronal responsiveness in cat visual cortex. *Nature, 368*(6474), 847–850.

Sengpiel, F., Sen, A., & Blakemore, C. (1997). Characteristics of surround inhibition in cat area 17. *Experimental Brain Research, 116*(2), 216–228.

Simoncelli, E. P., & Heeger, D. J. (1998). A model of neuronal responses in visual area MT. *Vision Research, 38*(5), 743–761.

Snowden, R. J., & Hammett, S. T. (1992). Subtractive and divisive adaptation in the human visual system. *Nature, 355*(6357), 248–250.

Stromeyer, C. F., Kronauer, R. E., Madsen, J. C., & Klein, S. A. (1984). Opponent mechanisms in human vision. *Journal of the Optical Society of America A, 1*, 876–884.

Thomas, J. P., & Olzak, L. A. (1997). Contrast gain control and fine spatial discriminations. *Journal of the Optical Society of America A Optics & Image Science, 14*(9), 2392–2405.

Toth, L. J., Rao, S. C., Kim, D. S., Somers, D., & Sur, M. (1996). Subthreshold facilitation and suppression in primary visual cortex revealed by intrinsic signal imaging. *Proceedings of the National Academy of Sciences of the United States of America, 93*(18), 9869–9874.

van Santen, J. P., & Sperling, G. (1984). Temporal covariance model of human motion perception. *Journal of the Optical Society of America, 1*(5), 451–473.

van Wezel, R. J., Lankheet, M. J., Verstraten, F. A., Maree, A. F., & van de Grind, W. A. (1996). Responses of complex cells in area 17 of the cat to bi-vectorial transparent motion. *Vision Research, 36*(18), 2805–2813.

Watson, A. B., & Ahumada, A. J., Jr. (1985). Model of human visual-motion sensing. *Journal of the Optical Society of America, 2*(2), 322–342.

Watson, A. B., & Solomon, J. A. (1997). Model of visual contrast gain control and pattern masking. *Journal of the Optical Society of America A Optics & Image Science, 14*(9), 2379–2391.

Wilson, H. R., Ferrera, V. P., & Yo, C. (1992). A psychophysically motivated model for two-dimensional motion perception. *Visual Neuroscience, 9*(1), 79–97.

Wilson, H. R., & Humanski, R. (1993). Spatial frequency adaptation and contrast gain control. *Vision Research, 33*(8), 1133–1149.

Wilson, H. R., McFarlane, D. K., & Phillips, G. C. (1983). Spatial frequency tuning of orientation selective units estimated by oblique masking. *Vision Research, 23*(9), 873–882.

Xing, J., & Heeger, D. J. (2000). Center surround interactions in foveal and peripheral vision. *Vision Research, 40*(22), 3065–3072.

Zemany, L., Stromeyer, C. F., Chaparro, A., & Kronauer, R. E. (1998). Motion detection on flashed, stationary pedestal gratings: evidence for an opponent-motion mechanism. *Vision Research, 38*(6), 795–812.